



# The Bolcana Cu–Au ore deposit (Metaliferi Mountains, Romania): first data on the alteration and related mineralisation

Viorica Milu, Jacques L Leroy, Patrice Piantone

## ► To cite this version:

Viorica Milu, Jacques L Leroy, Patrice Piantone. The Bolcana Cu–Au ore deposit (Metaliferi Mountains, Romania): first data on the alteration and related mineralisation. Comptes Rendus. Géoscience, 2003, 335 (8), pp.671 - 680. 10.1016/s1631-0713(03)00120-2 . hal-04082508

HAL Id: hal-04082508

<https://brgm.hal.science/hal-04082508>

Submitted on 26 Apr 2023

**HAL** is a multi-disciplinary open access archive for the deposit and dissemination of scientific research documents, whether they are published or not. The documents may come from teaching and research institutions in France or abroad, or from public or private research centers.

L'archive ouverte pluridisciplinaire **HAL**, est destinée au dépôt et à la diffusion de documents scientifiques de niveau recherche, publiés ou non, émanant des établissements d'enseignement et de recherche français ou étrangers, des laboratoires publics ou privés.



Available online at [www.sciencedirect.com](http://www.sciencedirect.com)



C. R. Geoscience 335 (2003) 671–680



## Geomaterials (Ore deposits)

# The Bolcana Cu–Au ore deposit (Metaliferi Mountains, Romania): first data on the alteration and related mineralisation

Viorica Milu<sup>a</sup>, Jacques L. Leroy<sup>b,\*</sup>, Patrice Piantone<sup>c</sup>

<sup>a</sup> Department of Mineral Resources, Geological Institute of Romania, 1 Caransebes Str., 78344-Bucharest, Romania

<sup>b</sup> UMR G2R, université Henri-Poincaré – Nancy-I, BP 239, 54506 Vandoeuvre-lès-Nancy cedex, France

<sup>c</sup> BRGM, DR/REM, BP 6009, 45060 Orléans cedex 2, France

Received 7 October 2002; accepted 23 June 2003

Presented by Zdenek Johan

## Abstract

The Bolcana ore deposit (Metaliferi Mountains, western Romania) is a porphyry ore deposit with associated epithermal veins. On the basis of different parageneses, four alteration types were distinguished: potassic, phyllitic, argillitic and propylitic. The mineralogical and geochemical data and estimated crystallisation temperatures of alteration minerals indicate an evolution of the system from an early period of porphyry type mineralisation (Cu + Au) to a late period of low-sulphidation epithermal mineralisation (Au + base metal). **To cite this article:** V. Milu et al., C. R. Geoscience 335 (2003).

© 2003 Académie des sciences. Published by Éditions scientifiques et médicales Elsevier SAS. All rights reserved.

## Résumé

**Le gisement de cuivre-or de Bolcana (monts Métallifères, Roumanie) : premières données sur les altérations et minéralisations associées.** Le gisement de Bolcana (monts Métallifères, Roumanie occidentale) est un gisement de type porphyre, associé à des veines épithermales, dans lequel les quatre types d'altération caractéristiques, potassique, phylliteuse, argileuse et propylitique, ont été reconnus à partir des différentes associations minérales rencontrées. Les analyses minéralogiques et géochimiques ainsi que les températures de cristallisation estimées des minéraux d'altération indiquent une évolution du système depuis une période initiale de minéralisation à cuivre-or de type porphyre jusqu'à une minéralisation épithermale à or-métaux de base de type *low-sulphidation*. **Pour citer cet article :** V. Milu et al., C. R. Geoscience 335 (2003).

© 2003 Académie des sciences. Published by Éditions scientifiques et médicales Elsevier SAS. All rights reserved.

**Keywords:** Cu–Au ore deposit; porphyry-epithermal deposit; hydrothermal alteration; geothermometer; Metaliferi Mountains; Romania

**Mots-clés :** gisements de cuivre-or ; gisement de type porphyre-épithermal ; altérations hydrothermales ; géothermomètres ; monts Métallifères ; Roumanie

\* Corresponding author.  
E-mail address: jacques.leroy@g2r.uhp-nancy.fr (J.L. Leroy).

## Version française abrégée

### 1. Introduction

Quatorze gisements et occurrences de type porphyre à Cu et Cu–Au sont connus dans les monts Métallifères (Ouest de la Roumanie), parmi lesquels le gisement de Bolcana, situé à une quinzaine de kilomètres au nord-est de la ville de Deva (Fig. 1A). Ce gisement est connu et étudié depuis le début des années 1970 [5,6,32–34].

Le gisement de Bolcana appartient au district métallogénique néogène de Brad–Sacaramb (Fig. 1A). Dans la région de Bolcana, le magmatisme néogène débute par les andésites de Hondol–Faerag, d'âge Sarmatien (Fig. 1B). L'intrusion de Bolcana, de composition microdioritique, intrude ces andésites dans la partie centrale de la zone volcanique Dumbravita–Teascu–Faerag [9]. Ce corps sub-volcanique a été exploré jusqu'à une profondeur de 1300 m. Des brèches polygéniques à éléments d'ophiolite et d'andésite sont observées autour de celui-ci. Les produits volcaniques les plus récents sont représentés par des andésites quartzeuses dépourvues de minéralisation [5].

L'objectif de ce travail est de caractériser les paragenèses d'altération, leurs relations avec la minéralisation et d'utiliser leurs caractéristiques pour en estimer les températures de cristallisation.

### 2. Minéralisation

Bolcana est un gisement de type porphyre à Cu–Au, associé à des veines de type épithermal. La minéralisation de type porphyre est localisée dans le corps subvolcanique de Bolcana et est constituée de chalcopyrite, pyrite, bornite, magnétite, hématite, molybdénite, avec de l'or principalement en inclusions dans la chalcopyrite. L'extension maximale du corps minéralisé (750 m × 440 m) se situe au niveau de l'horizon de Grimm, à l'altitude de 320 m (Fig. 1B). La minéralisation épithermale recoupe les roches altérées et minéralisées du type porphyre. Elle consiste en pyrite, sphalerite, galène, chalcopyrite, tétraédrite, bournonite, marcasite, or natif, arsénopyrite. Elle apparaît sous la forme de veines polymétalliques à gangue de carbonates et de veines à quartz aurifère [32,33]. Le forage F4 (Figs. 1B et 2) permet d'observer une coupe de 1000 m dans les roches altérées et minéralisées.

Les teneurs en Cu (0,11 pds % à 0,74 pds %) et Au (0,09 à 1,06 g t<sup>-1</sup>) augmentent avec la profondeur et sont maximales dans la zone d'altération potassique ± phylliteuse. Minéralisation à Cu, altération hydrothermale (potassique) et intrusion de Bolcana sont liées spatialement. Les analyses à l'échelle du gisement montrent que Au et Cu sont corrélés, mais qu'il n'y a pas de corrélation entre ces éléments et Mo.

### 3. Altérations hydrothermales

Quatre types d'altération ont été reconnus. L'altération potassique (Fig. 2) s'est développée dans la partie interne et profonde de l'intrusion et passe progressivement à l'altération phylliteuse, puis argileuse, ou brutalement à cette dernière. La biotite et le feldspath potassique en sont les principaux minéraux caractéristiques, avec chlorite, anhydrite, actinote, albite et séricite. L'altération phylliteuse s'est développée plus haut dans la structure et est caractérisée par illite, phengite, interstratifiés illite–smectite, quartz et pyrite, avec chlorite et anhydrite subordonnées. L'altération argileuse déborde largement autour de l'intrusion. Les minéraux caractéristiques sont kaolinite, smectite, interstratifiés et carbonates (« altération argileuse intermédiaire »). L'altération propylitique est la plus externe et affecte principalement l'andésite de Hondol–Faerag. Elle est caractérisée par l'assemblage chlorite, epidote, actinote, avec séricite et carbonates subordonnés. En surface, une altération supergène se développe, conduisant à la formation de kaolinite, halloysite, Fe-(hydr)oxydes, Na-jarosite, etc.

Avec des valeurs de  $X_{\text{Fe}}$  comprises entre 0,27 et 0,31 et de  $\text{Al}^{\text{VI}}$  entre 0,16 to 0,35 (formule calculée sur la base de 11 oxygènes), les biotites formées sont dans le champ des Mg-biotites [13]. Les chlorites sont toutes des clinochlores [1,12] ( $X_{\text{Fe}}$  entre 0,32 et 0,47;  $\text{Si}_{2.71}\text{Al}_{1.29}$  à  $\text{Si}_{2.95}\text{Al}_{1.05}$ ). Les minéraux phylliteux sont des phengite, illite, interstratifiés illite–smectite (IS and ISII) et K-smectite (Tableau 1), avec un continuum des phengites à la K-smectite (Fig. 3) [18].

### 4. Géothermomètres

Différents géothermomètres ont été utilisés (Tableau 2) afin d'approcher les températures de formation des minéraux d'altération. Ainsi, des températures de 350–450 °C ont été calculées pour la biotite à l'aide

de la courbe de solubilité de  $Ti^{4+}$  en fonction de la température [22], conformément aux données de la littérature [2,11], 265–355 °C pour les chlorites [7,8], les températures les plus élevées correspondant à des chlorites en veine, 230–260 °C pour les illites [7].

### 5. Discussion

Une diminution des températures de formation des biotites aux chlorites et aux illites, conforme aux données de la littérature [14,28,36] a été déterminée à l'aide des géothermomètres minéraux. Cette baisse de température est également indiquée par l'évolution minéralogique continue des phengites aux K-smectites (Fig. 3). En prenant en compte les zones d'altération observées et leurs relations spatio-temporelles, les températures estimées, ainsi que le domaine de stabilité des minéraux caractéristiques [14,19,21,35], l'altération hydrothermale développée à Bolcana est interprétée comme le résultat de la superposition de plusieurs types d'altération distincts. L'altération propylitique apparaît comme synchrone de l'altération potassique, mais plus externe. L'altération phylliteuse est postérieure à l'altération potassique et a probablement formé un halo limité autour de l'intrusion de Bolcana. L'altération argileuse se superpose à l'ensemble des altérations.

Cette étude indique également l'association à Bolcana de deux systèmes, un système porphyre, tout à fait comparable à d'autres systèmes porphyres [23,25], et un système épithermal caractéristique des systèmes de type *low sulphidation*. Les stades précoce correspondent à une minéralisation de type porphyre à Cu–Au en relation, principalement, avec le développement de l'altération potassique. Dans les stades tardifs, des filons épithermaux à or–métaux de base recoupent les minéralisations et altérations porphyriques. Cette association spatiale entre système porphyrique à Cu (Au) et système épithermal de type *low-sulphidation* a été décrit en différents sites, comme en Papouasie-Nouvelle-Guinée (Ladolam) [27].

### 1. Introduction

The Metaliferi Mountains (western Romania) host 14 Neogene porphyry Cu and Cu–Au ore deposits and occurrences, including the Bolcana Cu–Au deposit.

The Bolcana deposit belongs to the Brad-Sacaramb metallogenic district and is located approximately 15 km northeast of the town of Deva (Fig. 1A). The ore deposit has been identified and studied starting in the early 1970s and these studies resulted in important contributions [5,6,32–34]. However, there is no published data concerning the chemical composition of minerals associated with the Bolcana deposit.

This paper discusses both alteration and mineralization styles. The hydrothermal minerals are used to determine: (1) mineral assemblages and the alteration types; (2) relationships between alteration and mineralization; (3) alteration patterns. Mineral chemistry of some alteration minerals was used in order to estimate their crystallization temperatures.

### 2. Methods

Mineralogical studies were performed on samples collected from outcrops, exploration galleries and drill cores. Thin and polished thin sections were examined by optical microscopy. Mineral analyses were carried out using a Camebax–SX50 electron microprobe with a wavelength-dispersive spectrometer. Operating conditions: acceleration voltage was 15 kV, counting time 6 s, sample current of 12 nA. Analysed elements: Si, Al, Fe, Mg, Mn, K, Ca, Ti, and Cr ( $\pm$ Sr, Cl). X-ray diffraction analyses on whole rock samples and on argillic fractions were performed using a Siemens D5000 diffractometer. Major and trace elements were analysed by inductively coupled plasma (ICP) methods and Au by atomic absorption spectrophotometry (AAS). All these analyses were carried out at BRGM (Orléans, France) and at the Henri-Poincaré University (Nancy, France).

### 3. Geological setting

Neogene calc-alkaline magmatic activity is known to have started in western Romania at about 15 Ma and continued up to 7.4 Ma. After a gap of about 6 Ma, a more alkaline type activity is recorded [29,30].

The Bolcana deposit belongs to the Neogene Brad-Sacaramb metallogenic district (Fig. 1A). The basement of the area consists of Middle Jurassic–Lower Cretaceous ophiolitic rocks (basaltic andesites and

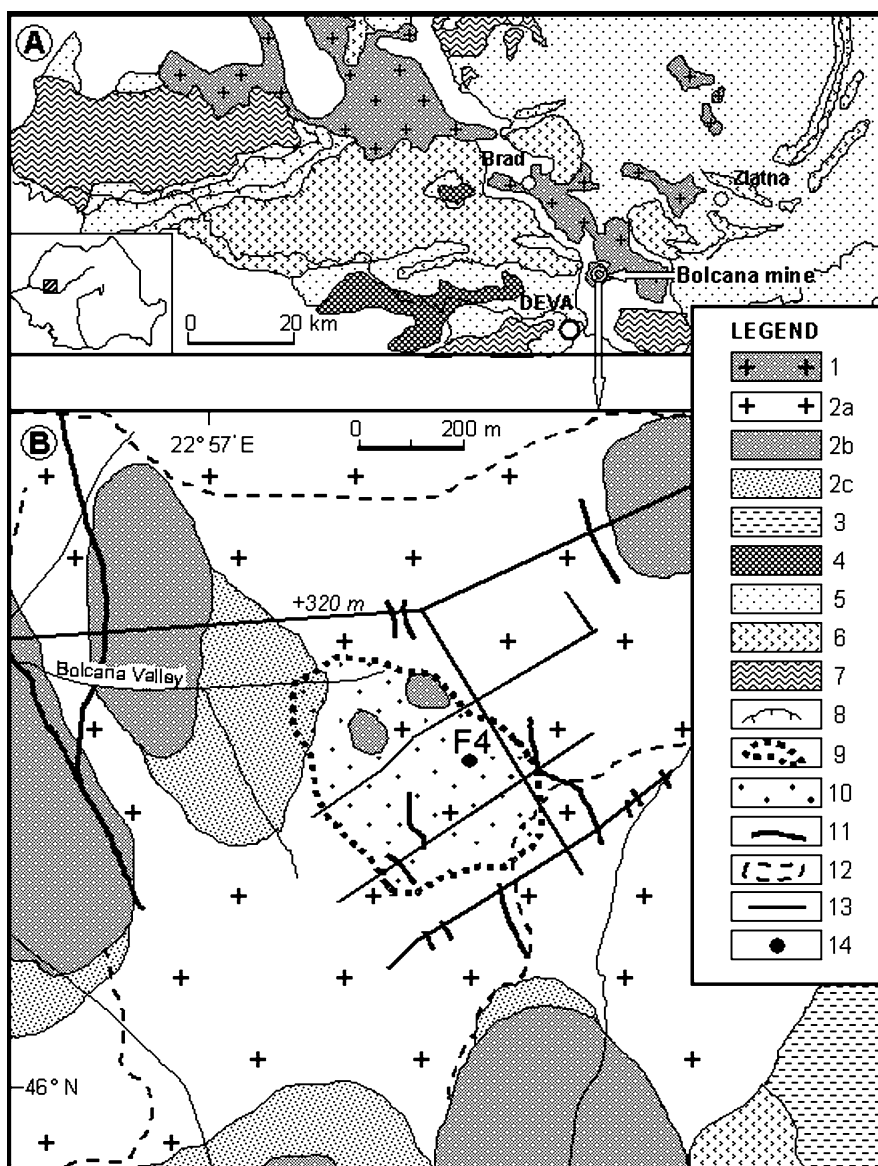


Fig. 1. **A.** Simplified geological map of the Metaliferi Mountains showing the location of the studied area (after [10]). **B.** Geological map of the Bolcana mining area (after [33,34] with modifications). Location of F4 drill-hole is indicated. **1.** Neogene magmatic rocks. **2.** Upper Badenian–Sarmatian andesites-microdiorites (**2a**, lavas and pyroclastics; **2b**, bodies; **2c**, breccia); **3.** Paleocene sedimentary rocks; **4.** Upper Cretaceous–Paleocene magmatic rocks; **5.** Mesozoic sedimentary rocks; **6.** Mesozoic ophiolites; **7.** Pre-alpine undifferentiated rocks; **8.** overthrust; **9.** limit of the Bolcana porphyritic intrusion at the level +320 m above sea level (Grimm exploration level); **10.** Porphyry copper mineralization; **11.** epithermal vein; **12.** limit of the area with altered rocks; **13.** exploration galleries at the Grimm level; **14.** drill-hole.

Fig. 1. **A.** Carte géologique simplifiée des monts Métallifères, montrant la localisation de la zone étudiée (d'après [10]). **B.** Carte géologique de la zone minière de Bolcana (modifiée d'après [33,34]), avec localisation du forage F4. **1.** Roches magmatiques néogènes ; **2.** Andésites-microdiorites du Badénien–Sarmatien supérieur (2a, laves et pyroclastites ; 2b, corps ; 2c, brèches) ; **3.** roches sédimentaires du Paléocène ; **4.** roches magmatiques du Crétacé supérieur-Paléocène ; **5.** roches sédimentaires mésozoïques ; **6.** ophiolites mésozoïques ; **7.** roches indifférenciées pré-alpines ; **8.** chevauchement ; **9.** limite de l'intrusion porphyrique de Bolcana au niveau +320 m au-dessus du niveau de la mer (niveau d'exploration Grimm) ; **10.** minéralisation de type porphyre Cu ; **11.** veines épithermales ; **12.** limite de l'altération ; **13.** galeries d'exploration au niveau Grimm ; **14.** forage.

basalts lava flows and pyroclastics) and Lower Cretaceous rhyolites (Baita rhyolites) overlain by Palaeocene sedimentary series (Almasul Mare Formation), composed of gravels, sands and silty clays [3,4], and sedimentary series of Middle Miocene age, consisting of clays, sands and gravels outcropping unconformably [24]. In the area of Bolcana, the oldest Neogene igneous rocks are represented by andesites that occur as lava flows, intrusions and pyroclastics (Fig. 1B). They are of Sarmatian age and are known as Hondol-Faerag andesites. A subvolcanic body (Bolcana intrusion) of microdioritic composition intrudes these andesites. The Bolcana intrusion is located in the central part of the Dumbravita–Teascu–Faerag Neogene volcanic zone [9] and it outcrops only in a small area. The Bolcana intrusion was explored down to 1300 m in depth. Intrusive polymictic breccias, with ophiolitic and Neogene andesitic elements, are observed around this subvolcanic body. The youngest volcanic products comprise quartz andesites, but they are devoid of mineralisation [5].

#### 4. Mineralisation

Bolcana is a porphyry-type Cu–Au ore deposit with associated epithermal veins. The porphyry Cu–Au mineralisation is located in the Bolcana subvolcanic body and is represented by chalcopyrite, pyrite, bornite, magnetite, hematite, molybdenite, with subordinate gold (mainly as inclusions in chalcopyrite). Chalcopyrite is the dominant copper mineral. The maximum extension of the orebody (750/440 m) is observed at the Grimm horizon (level +320 m) (Fig. 1B). At the same horizon, the distribution of the epithermal veins is also presented. The veins cut the early altered and mineralised rocks. The epithermal mineralisation consists of pyrite, sphalerite, galena, chalcopyrite, tetrahedrite, bournonite, marcasite, native gold, arsenopyrite and pyrrhotite [32,33]. There are poly-metallic veins with predominantly carbonate gangue and gold-bearing quartz veins; illite and mixed-layer minerals also form in and envelop these veins.

The F4 drill-hole (Fig. 1B), carried out by the MINEXFOR Company, provides 1000 m long section in altered and mineralisation-rich rocks. Within the mineralised section (Fig. 2), the Cu content ranges from 0.11 to 0.74 wt%, and the gold content varies

from 0.09 to 1.06 g t<sup>-1</sup>. The Mo content varies from 7 to 38 g t<sup>-1</sup>; a higher Mo content (272 g t<sup>-1</sup>) was found in a sample with molybdenite vein located at the depth of 781 m. Whole-rock analyses indicate that Cu is positively correlated with Au, whereas there is no correlation between these elements and Mo. The Cu and Au concentrations increase with depth and the high-grade ore is located within the Bolcana intrusion affected by potassic ± phyllitic alteration (Fig. 2). Many gold-bearing porphyry copper deposits have a close correlation between the gold grade and copper grade in the potassic alteration zone [20,31].

### 5. Hydrothermal alteration

#### 5.1. Mineral assemblages and alteration types

The chemical compositions (average values) and structural formulae of some alteration minerals from Bolcana deposit are given in Table 1. In this deposit, the potassic alteration is dominated by secondary biotite that occurs mainly as replacement biotite (resulting from the alteration of primary hornblende and plagioclase) and disseminated biotite (fine aggregates in the groundmass). The presence of secondary biotite is restricted to the subvolcanic body. All the analysed biotites show an  $X_{\text{Fe}}$  ratio ranging between 0.27 and 0.31; the  $\text{Al}^{\text{VI}}$  values vary from 0.16 to 0.35 (structural formula calculated on the basis of 11 oxygens).  $\text{Mg}/(\text{Mg} + \text{Fe})$  and  $\text{Al}^{\text{VI}}$  values indicate Mg-biotite [13]. Plagioclase retains its original forms but usually is more or less altered toward a variable assemblage including K-feldspar (e.g.,  $\text{Or}_{74}\text{Ab}_{23}$ ), albite, and phyllitic minerals. Albite appears either as a rim around the more or less albited primary plagioclase, or as veinlets or being disseminated in the altered rock. Chlorites, collected both from exploration galleries and drill-cores at different depths, are systematically clinochlore [1,12] and have a restricted compositional range. Their  $X_{\text{Fe}}$  molar ratio varies from 0.32 to 0.47 (the average: 0.39; Table 1) and the Si and Al occupancy in tetrahedral sites varies from  $\text{Si}_{2.71}\text{Al}_{1.29}$  to  $\text{Si}_{2.95}\text{Al}_{1.05}$ .

Furthermore, microprobe and XRD analyses indicate the presence of various phyllitic minerals, like phengite, illite, illite-smectite mixed-layer minerals (IS and ISII) and K-smectite (Table 1). In Fig. 3, the

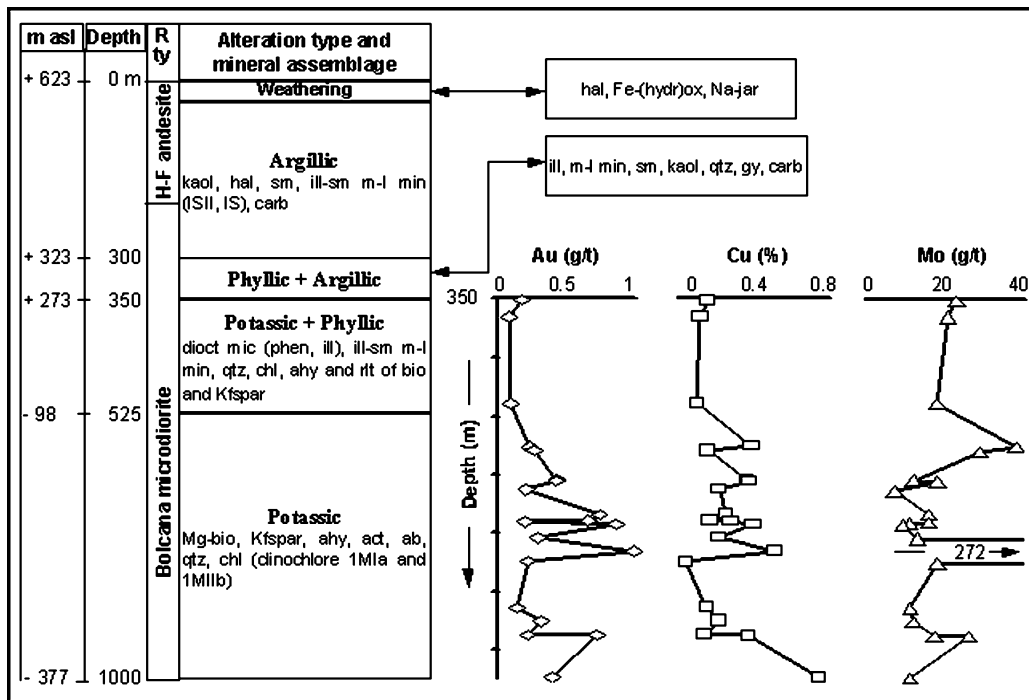


Fig. 2. Synthetic column of F4 drill-hole, showing the characteristic mineral assemblages and the alteration types. The variation of Cu, Au and Mo contents in drillcore samples are also represented (content vs. depth diagram). *ab*, albite; *act*, actinolite; *ahy*, anhydrite; *bio*, biotite; *carb*, carbonates; *chl*, chlorite; *dioc mic*, diocatahedral micas; *Fe-(hydr)ox*, Fe-(hydr)oxydes; *gp*, gypsum; *H-F*, Hondol-Faerag; *hal*, halloysite; *ill*, illite; *IS*, illite/smectite; *ISII*, illite/smectite/illite/illite; *kaol*, kaolinite; *Kfspar*, K-feldspar; *m asl*, metres above sea level; *Mg-bio*, Mg-biotite; *min*, minerals; *m-l*, mixed-layer; *Na-jar*, Na-jarosite; *phen*, phengite; *qtz*, quartz; *R ty*, rock type; *rtl*, relicts; *sm*, smectite.

Fig. 2. Log synthétique du forage F4, montrant les assemblages minéralogiques caractéristiques, les types d'altération, ainsi que les variations des teneurs en Cu, Au et Mo en fonction de la profondeur. *ab*, albite ; *act*, actinote ; *ahy*, anhydrite ; *bio*, biotite ; *carb*, carbonates ; *chl*, chlorite ; *dioc mic*, mica diocataédrique ; *Fe-(hydr)ox*, Fe-(hydr)oxydes ; *gp*, gypse ; *H-F*, Hondol-Faerag ; *hal*, halloysite ; *ill*, illite ; *IS*, illite/smectite ; *ISII*, illite/smectite/illite/illite ; *kaol*, kaolinite ; *Kfspar*, feldspath K ; *m asl*, altitude (en m) au-dessus du niveau de la mer ; *Mg-bio*, Mg-biotite ; *min*, minéraux ; *m-l*, minéraux interstratifiés ; *Na-jar*, Na-jarosite ; *phen*, phengite ; *qtz*, quartz ; *Rty*, type de roche ; *rtl*, reliques ; *sm*, smectite.

K content in interlayer site and the interlayer charge values of these minerals were plotted in a discrimination diagram [18]. As it can be seen, both the terms of illite-smectite series and the smectites are dominantly potassic, with a continuous mineralogical variation from phengite to K-smectite.

On the basis of different parageneses, four alteration types were distinguished [26]: potassic, phyllitic, argillic and pyrophytic.

The *potassic alteration* is developed in the deepest and innermost part of the intrusive body; it grades upward either to phyllitic and then to argillic alteration or directly to the argillic alteration type. Drillings carried out within the core of the porphyry intrusion

indicate that potassic alteration still occurs at the depth of 1000 m (e.g., F4-drill hole, Fig. 2). Mg-biotite and K-feldspar are the main minerals; chlorite (clinochlore 1M1a and 1M1b), anhydrite, actinolite, albite and sericite are also present.

The *phyllitic alteration* is less developed and the characteristic minerals either crystallized in veinlets or replaced the pre-existing minerals in wall rocks. The phyllitic assemblage consists of sericite, quartz and pyrite, with subordinate chlorite, anhydrite and relicts of biotite and K-feldspar. In the description of this alteration type, we use the term ‘sericite’ in the sense to include both illite and illite-smectite mixed-layer minerals [15,16].

Table 1

Electron microprobe analyses (wt%) and structural formulae of some alteration minerals from Bolcana deposit. Structural formulae of minerals have been calculated on a basis of 11 oxygens, except for chlorite, whose formulae have been calculated on a basis of 14 oxygens. *IS*, illite-smectite mixed layer minerals; *ISII*, illite-smectite-illite-illite mixed layer minerals; *n*, number of analyses averaged;  $X_{\text{Fe}} = \text{Fe}/(\text{Fe} + \text{Mg})$ ; \* $\Sigma\text{Fe}$  determined as FeO

Tableau 1

Composition chimique (moyenne en poids %, microsonde électronique) et formule structurale de quelques minéraux d'altération du gisement de Bolcana. Les formules structurales sont calculées sur la base de 11 oxygènes et de 14 oxygènes pour les chlorites. *IS*, minéraux interstratifiés illite-smectite ; *ISII*, minéraux interstratifiés illite-smectite-illite-illite ; *n*, nombre d'analyses utilisées ;  $X_{\text{Fe}} = \text{Fe}/(\text{Fe} + \text{Mg})$  ; \* $\Sigma\text{Fe}$  déterminé sous la forme de FeO

<i>n</i>	Biotite 4	Chlorite 15	Phengite 3	Illite 7	<i>IS</i> 6	<i>ISII</i> 2	Smectite 4
SiO <sub>2</sub>	37.25	27.94	49.00	48.32	48.74	48.04	51.92
Al <sub>2</sub> O <sub>3</sub>	16.51	20.29	31.11	30.30	31.17	28.79	35.13
Cr <sub>2</sub> O <sub>3</sub>	0.01	0.02	0.00	0.02	0.00	0.10	0.05
TiO <sub>2</sub>	2.23	0.07	0.05	0.05	0.04	0.01	0.04
FeO*	11.91	19.64	2.47	3.27	3.29	4.40	1.08
MgO	16.44	18.03	1.83	2.29	2.37	4.10	0.60
MnO	0.21	0.34	0.08	0.07	0.03	0.15	0.05
K <sub>2</sub> O	9.38	0.14	10.12	8.49	6.37	7.44	3.67
Na <sub>2</sub> O	0.19	0.01	0.33	0.22	0.07	0.08	0.04
CaO	0.01	0.12	0.08	0.19	0.17	0.16	0.11
Total	94.15	86.61	95.07	93.20	92.25	93.27	92.69
Si <sup>IV</sup>	2.77	2.88	3.27	3.27	3.28	3.25	3.35
Al <sup>IV</sup>	1.23	1.12	0.73	0.73	0.72	0.75	0.65
Al <sup>VI</sup>	0.21	2.09	1.71	1.69	1.75	1.55	2.02
Cr	0.00	0.00	0.00	0.00	0.00	0.01	0.00
Ti	0.12	0.01	0.00	0.00	0.00	0.00	0.00
Fe	0.74	2.65	0.14	0.19	0.19	0.25	0.06
Mg	1.82	4.16	0.18	0.23	0.24	0.43	0.06
Mn	0.01	0.05	0.00	0.00	0.00	0.01	0.00
K	0.91	0.03	0.88	0.75	0.56	0.66	0.31
Na	0.03	0.00	0.04	0.03	0.01	0.01	0.01
Ca	0.00	0.03	0.01	0.01	0.01	0.01	0.01
$X_{\text{Fe}}$	0.29	0.39	0.43	0.44	0.41	0.45	0.51

The *argillic alteration* is developed in the upper part of the Bolcana ore-forming system and it affected both the porphyritic body and associated intrusion breccias, and the host rocks. The mineral assemblage corresponds to the intermediate argillic alteration type, characterized by the presence of kaolinite, smectite, mixed-layer minerals and carbonates. Fissures filled with minerals characteristic of the phyllitic and argillic alterations crosscut even the deeper part of the porphyritic intrusion. In the argillic alteration zone, relicts of phyllitic-altered rocks occur.

The *propylitic alteration* affected mainly the Hon-dol-Faerag andesites and occurs either like a broad halo around the other alteration types, or as relict

islands in the argillic alteration zone. Propylitized rocks consist of chlorite, epidote, actinolite, and minor sericite and carbonates, which replaced plagioclase and mafic minerals.

A large development of sulphidation [32] and carbonatation (calcite) is a peculiarity of the Bolcana hydrothermal system. Anhydrite, often replaced by gypsum (especially where phyllitic + argillic alteration overprints the potassic alteration), occurs both in the veinlets and groundmass.

At the surface, supergene alteration is developed. This type of alteration is characterized by the occurrence of kaolinite, halloysite, Fe-(hydr)oxides, Na-jarosite, etc.

Table 2

Ranges of crystallisation temperatures of biotite, chlorite and illite from Bolcana ore deposit. *bio*, biotite; *chl*, chlorite; *chl 1*, chl in veinlet; *chl 2* chl in groundmass; *chl 3* chlorite on phenocrysts; *ill* illite; *rpl* replacement

Tableau 2

Intervalle de température de formation des biotite, chlorite et illite néoformées du gisement de Bolcana. *bio*, biotite ; *chl*, chlorite ; *chl 1*, chl en veineule ; *chl 2*, chl dans la masse ; *chl 3*, chlorite sur phénocristaux ; *ill*, illite ; *rpl*, remplacement

Geothermometer	Crystallisation temperature (°C)
Biotite [19]	350–450 ( <i>rpl bio</i> )
Chlorite [7,8]	345–355 ( <i>chl 1</i> )
Illite [7]	230–260 ( <i>rpl ill</i> )
	285–320 ( <i>chl 2</i> )
	265–272 ( <i>chl 3</i> )

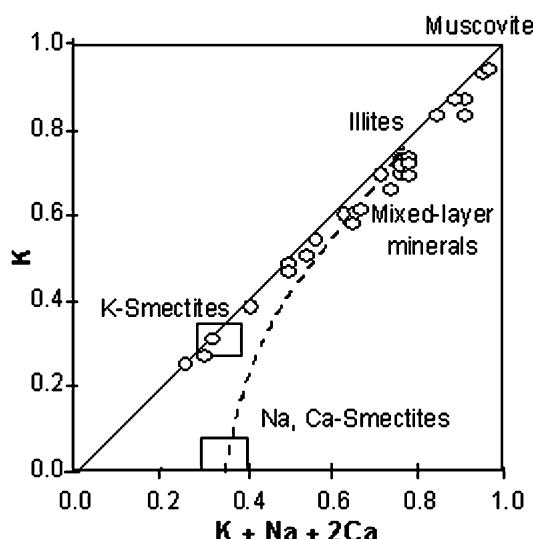


Fig. 3. ( $K + Na + 2 Ca$ ) vs.  $K$  diagram (from [17]).

Fig. 3. Diagramme ( $K + Na + 2 Ca$ ) vs.  $K$  [17].

## 5.2. Mineral geothermometry

Using the calculated structural formulae of some alteration minerals, their crystallisation temperatures were estimated applying different geothermometers (Table 2): the illite geothermometer using its K-interlayer content [7], the chlorite geothermometer [7,8] applied to different types of chlorites (formed by alteration of mafic phenocrysts and groundmass, and crystallized in veinlets), the solubility curve of  $Ti^{4+}$  as a function of temperature [22] for secondary biotite.

Geothermometry, based on biotite composition, indicates temperatures in the range 350–450 °C for the formation of a replacement biotite, similar to the crystallisation temperatures of biotite from other porphyry copper deposits (e.g., Santa Rita, New Mexico; Ray

and Safford, Arizona; Panguna, Papua New Guinea) [2,11].

The composition of chlorite from Bolcana indicates temperatures of formation between 265 and 355 °C. The highest calculated formation temperatures (345–355 °C) correspond to chlorite in veinlets and the calculated temperatures decrease from chlorite in veinlet to chlorite formed in groundmass and to chlorite formed from phenocrysts.

Applying the illite geothermometer, a temperature range from 230 to 260 °C was obtained for the replacement illite, formed in groundmass.

## 6. Discussion

The continuous mineralogical variation from phengite to K-smectite, observed in Fig. 3, gives evidence of, and is related to the decrease of temperature and/or to the chemical evolution of the hydrothermal fluids in the system [17]. Concerning the estimated crystallisation temperatures of biotite, chlorite and illite (Table 2), a temperature decrease is observed from biotite to chlorite and illite. The thermometric data are consistent with the crystallization temperatures of these minerals [14,28,36]. Taking into consideration the values obtained and also the alteration zones and the stability domains of specific minerals [14,19,21,35], the alteration pattern at Bolcana is considered as the result of an overprinting of alteration processes. Propylitisation seems to be nearly simultaneous with, but peripheral to, the potassic alteration. Phyllitic alteration is posterior to the potassic alteration and is supposed to have formed a reduced halo around the Bolcana intrusion. Argillic alteration overprints the other alteration types.

At Bolcana, both porphyry and epithermal systems are distinguished. The alteration assemblages asso-

ciated to porphyry copper mineralisation are similar to those described in other porphyry copper systems [23,25]. The potassic alteration and porphyry copper mineralisation are spatially related and are thought to be formed almost at the same stage with the likelihood that the mineralisation process continued during later alteration processes. In the epithermal veins, mineralisation and alteration assemblages are characteristic of a low-sulphidation epithermal type mineralisation.

The paragenetic studies indicate an evolution of the system from an early period of porphyry Cu–Au mineralisation (mainly chalcopyrite, pyrite, magnetite, hematite, bornite, and molybdenite, with subordinate native gold) to a late period of low-sulphidation epithermal mineralisation (pyrite, galena, chalcopyrite, tetrahedrite, marcasite, bournonite, arsenopyrite, pyrrhotite and native gold).

Therefore, the Bolcana deposit is characterized by a spatial association between a porphyry Cu (Au) and a low-sulphidation epithermal mineralization, as described in several places such as in Papua New Guinea (e.g., Ladolam) [27].

## Acknowledgements

The MININVEST and the MINEXFOR Companies are thanked for allowing accesses to their mines. Field support by E. Orlandea and D. Filipescu is acknowledged. We would like to thank Prof. Dr. E. Marcoux and an anonymous reviewer for their useful comments.

## References

- [1] P. Bayliss, Nomenclature of the trioctahedral chlorites, *Can. Mineral.* 13 (1975) 178–180.
- [2] R. Beane, Biotite stability in the porphyry copper environments, *Econ. Geol.* 69 (1974) 241–256.
- [3] M. Borcos, G. Popescu, E. Rosu, Nouvelles données sur la stratigraphie et l'évolution du volcanisme tertiaire des monts Métallifères, *DS Inst. Geol. Geophys.* 70–71 (1986) 245–259.
- [4] S. Bordea, M. Borcos, Geological map 73d – Brad. Sc. 1:50 000, *Inst. Geol.*, Bucharest, 1972.
- [5] S. Bostinescu, Porphyry copper systems in the South Apuseni Mountains – Romania, *Ann. Inst. Geol. Rom.* LXIV (1984) 163–175.
- [6] S. Bostinescu, C. Vlad, I. Bratosin, Étude des minéralisations de cuivre associées aux volcanites néogènes des monts Métallifères, en utilisant les données d'exploration – la zone Bolcana–Troita, *Geol. Inst. Rom.*, Bucharest, Report, 1980, 43 p., unpublished.
- [7] M. Cathelineau, Cation site occupancy in chlorites and illites as a function of temperature, *Clay Miner.* 23 (1988) 471–785.
- [8] M. Cathelineau, D. Nieva, A chlorite solid solution geothermometer: the Los Azufres (Mexico) geothermal system, *Contrib. Mineral. Petrol.* 91 (1985) 235–244.
- [9] G. Cioclica, G. Istrate, G. Popescu, G. Udubasa, Contributions to the knowledge of the volcanic product ages of the Hartagan-Trestia area, Metaliferi Mountains, *Stud. Cerc. Geol., Geofiz., Geogr.*, Ser. Geol. 11 (1) (1966) 171–182.
- [10] I. Dumitrescu, M. Sandulescu, Carte tectonique de la Roumanie, Échelle 1:1 000 000, *Inst. Geol.*, Bucharest, 1970.
- [11] J.H. Ford, A chemical study of alteration at the Panguna porphyry copper deposit, Bougainville, Papua New Guinea, *Econ. Geol.* 73 (1978) 703–720.
- [12] M.D. Foster, Interpretation of the composition and a classification of the chlorites, *Geol. Surv. Prof. Paper.* USA 414A (1962) 1–29.
- [13] C.V. Guidotti, Micas in metamorphic rocks, *Rev. Mineral.* 13 (1984) 357–467.
- [14] C.C. Harvey, P.R.L. Browne, Mixed layered clay geothermometry in the Wairakei geothermal Field, New Zealand, *Clay Miner.* 39 (1991) 614–621.
- [15] D.O. Hayba, P.M. Bethke, P. Heald, N.K. Foley, Geologic, mineralogic, and geochemical characteristics of volcanic-hosted epithermal precious-metal deposits, *Rev. Econ. Geol.* 2 (1985) 129–166.
- [16] P. Heald, N.K. Foley, D.O. Hayba, Comparative anatomy of volcanic-hosted epithermal deposits: acid-sulfate and adularia-sericite types, *Econ. Geol.* 82 (1987) 1–26.
- [17] J.J. Hemley, W.R. Jones, Chemical aspects of hydrothermal alteration with emphasis on hydrogen metasomatism, *Econ. Geol.* 64 (1969) 599–613.
- [18] J. Hower, T.C. Mowatt, The mineralogy of illites and mixed-layer illite/montmorillonite, *Am. Mineral.* 51 (1966) 825–854.
- [19] D. Jacobs, W. Parry, Geochemistry of biotite in the Santa Rita porphyry copper deposit, New Mexico, *Econ. Geol.* 74 (1979) 860–887.
- [20] B. Jones, Application of metal zoning to gold exploration in porphyry copper systems, *J. Geochem. Exploration* 43 (1992) 127–155.
- [21] T.M. Leach, C.P. Wood, A.G. Reyes, Hydrothermal alteration of the Tongonan geothermal field, Leyte, Philippines, in: Proc. 4th Int. Symp. on Water–Rock Reaction, Misima, Japan, 1983, pp. 275–278.
- [22] L. Le Bel, Études des conditions de formation du porphyre cuprifère de Cerro Verde–Santa Rosa (Pérou méridional) pris dans son contexte plutonique, thèse, université de Lausanne, BRGM, Orléans, 1979, 160 p.
- [23] J.D. Lowell, J.M. Guillet, Lateral and vertical alteration-mineralization zoning in porphyry ore deposits, *Econ. Geol.* 65 (1979) 373–408.
- [24] M. Lupu, H.G. Krautner, N. Ticleanu, S. Bostinescu, T. Brândrabur, F. Krautner, A.R. Horvath, I. Nicolae, Geological map 89b – Deva, *Inst. Geol. Geophys.*, Bucharest, 1982.

- [25] C. Meyer, in: H.L. Barnes (Ed.), *Geochemistry of Hydrothermal Ore Deposits*, Holt, Rinehart and Winston, New York, 1967, pp. 166–235.
- [26] V. Milu, Hydrothermal alteration associated with the Bolcana and Rosia Poieni porphyry copper deposits (South Apuseni Mountains), PhD thesis, Bucharest University, 1999, 250 p., in Romanian.
- [27] A.J. Moyle, B.J. Doyle, H. Hoogvliet, A.R. Ware, Ladolam gold deposit, Lihir Island, in: F.E. Hughes (Ed.), *Geology of the Mineral Deposits of Australia and Papua New Guinea*, Aust. Inst. Min. Metal. Monogr. (1990) 1793–1805.
- [28] A.G. Reyes, Petrology of Philippines geothermal systems and the application of alteration mineralogy to their assessment, *J. Volc. Geotherm. Res.* 43 (1990) 279–310.
- [29] E. Rosu, Z. Pecskay, A. Stefan, G. Popescu, C. Panaiotu, C.E. Panaiotu, The evolution of the Neogene volcanism in the Apuseni Mountains (Romania): constraints from new K–Ar data, *Geol. Carpathica* 48 (1997) 353–359.
- [30] E. Rosu, C. Panaiotu, Z. Pecskay, C.E. Panaiotu, Age, geochemistry, and evolution of Neogene magmatism in the Apuseni Mountains, Romania, Abs. ABCD-GEODE Workshop, Borovets, Bulgaria, 2000, p. 73.
- [31] R.H. Sillitoe, Some thoughts on gold-rich porphyry copper deposits, *Miner. Deposita* 14 (1979) 161–174.
- [32] G. Udubasa, G. Istrate, M. David, V. Neacsu, I. Bratosin, P. Andar, Étude métallogénique des minéralisations à Au–Ag et métaux non ferreux associées au volcanisme néogène des monts Métallifères : la zone Sacaramb–Baita, *Geol. Inst. Rom.*, Bucharest, Report, 1978, 27 p., unpublished.
- [33] G. Udubasa, A. Serbanescu, C. Vlad, I. Vanghelie, Étude des filons associés à la structure cuprifère Bolcana–Troita, *Geol. Inst. Rom.*, Bucharest, Report, 1981, 34 p., unpublished.
- [34] O. Vasilescu, S. Covaci, Étude minéralogique et pétrographique des minéralisations non ferreuses recoupées en travaux miniers et forages dans le périmètre Bolcana–Troita, le district Hunedoara, IPGG, Bucarest, Report, 1982, 45 p., unpublished.
- [35] B. Velde, Clay minerals: a physico-chemical explanation of their occurrences, *Dev. Sedimentol.* 40 (1985) 1–427.
- [36] D. Yates, P. Rosenberg, Formation and stability of endmember illite: I. Solution equilibration experiments at 100–250 °C and  $P_{v,soln}$ , *Geochim. Cosmochim. Acta* 60 (1996) 1873–1883.